Biomass and Bioenergy 134 (2020) 105469

Contents lists available at ScienceDirect

Biomass and Bioenergy

journal homepage: http://www.elsevier.com/locate/biombioe

Research paper

Fuel characterization and thermal degradation kinetics of biomass from phytoremediation plants

Khanh-Quang Tran [a,*], Sebastian Werle [b], Thuat T. Trinh [c], Aneta Magdziarz [d], Szymon Sobek [b], Marta Pogrzeba [e]

[a] Department of Energy and Process Engineering, Norwegian University of Science and Technology, Kolbjørn Hejes Vei 1B, Trondheim, Norway
[b] Silesian University of Technology, 22 Konarskiego St, 44-100, Gliwice, Poland
[c] Department of Civil and Environmental Engineering, Norwegian University of Science and Technology, NO-7491Trondheim, Norway
[d] AGH University of Science and Technology, Al. Mickiewicza 30, 30-059, Krakow, Poland
[e] Institute for Ecology of Industrial Areas, 6 Kossutha St, 40-844, Katowice, Poland

ARTICLE INFO

Keywords:
Fuel characterization
Thermal decomposition
Energy crops
Plant biomass
Sustainable phytoremediation

ABSTRACT

Biomass obtained from phytoremediation energy crops *Miscanthus* x *giganteus* and *Sida hermaphrodita* planted on different soils contaminated with heavy metals was thermogravimetrically studied and kinetically analyzed, assuming a three-pseudocomponent model. The results showed that *Miscanthus* x *giganteus* was able to uptake more heavy metals than *Sida hermaphrodita*. Soil influences on the fuel and thermal properties the crops were observed. The ash content of the biomass exhibited a negative effect on its reactivity. The extracted kinetic data are realistic and within reasonable ranges. The activation energies are within 20–103.55 kJ mol^{-1}. The reaction orders are within 1.01–1.99.

1. Introduction

Soil contamination is one of the major environmental problems worldwide, posing serious risks to environment and human health [1–3]. In the European Union for example there are approximately 3 million sites of soil suspected of being contaminated and 250,000 sites are known to require remediation [4]. Among these, the soils contaminated with heavy metals such as Cd, Cr, Pb, Cu, Zn, Co, Ni, Se, Cs and As account for more than 37% of the cases, followed by 33.7% for the contamination with mineral oil, 13.3% with polycyclic aromatic hydrocarbons and others [4]. In China, approximately 20% of the arable land is considered of being contaminated with heavy metals, posing deep global economic and geopolitical consequences for the international community in the coming years [5], considering the hazardous effects of heavy metals on the environment and human health when introduced into the food chain or by dust inhalation and swallowing of contaminated soil particles [3,6].

Remediation of soil contaminated with heavy metals presents distinct scientific and technical challenges, due to the fact that heavy metals cannot be degraded further into non-harmful products. Therefore, the only approach for the remediation is to remove or sequester the heavy metals from the soil. Current technological options available for remediation of soil contaminated with heavy metals include *in-situ* or *ex-situ* chemical treatment, biological treatment, soil washing, soil flushing, vitrification, incineration and landfilling [7].

As an in-situ biological treatment method, phytoremediation involves growing plants in contaminated sites to biologically extract and translocate the contaminants to the above-ground part of the plants for later harvest (*phytoextraction*); converting the metal elements to a less hazardous chemical speciation (*transformation*); or at the very least sequestering the elements in roots to prevent leaching from the sites (*phytostabilisation*).

Phytoremediation is a viable technology, offering a low cost alternative to physical and chemical treatment methods [8]. In addition, phytoremediation is an environmentally friendly technique because it decontaminates the contaminants along with the metabolism processes of plant species without disturbing the physical, chemical and ecological characteristics of the soil [9]. However, as a biological method, phytoremediation is limited by a number of factors such as the long treatment time, site and contaminant specificities. A key factor preventing the technology from large implementations is the disposal of large quantities of plant biomass materials contaminated with heavy metals

* Corresponding author.
E-mail address: khanh-quang.tran@ntnu.no (K.-Q. Tran).

https://doi.org/10.1016/j.biombioe.2020.105469
Received 25 February 2019; Received in revised form 3 January 2020; Accepted 10 January 2020
Available online 24 January 2020

accumulated throughout the remediation process [10,11]. When the contaminant content of plant biomass exceeds a specific level, the biomass is regarded as potentially hazardous material and therefore must be stored or disposed of appropriately [12]. To address this disposal problem, an integrated approach combining with post-processing of biomass from phytoremediation plants for recovery of energy and high value elements was proposed [1]. A model was developed to assess the viability of the proposed approach. It was concluded from this work that post-process energy and element recovery from biomass would significantly increase the financial viability of phytoremediation projects and reduce the environment impacts of disposal for contaminated biomass [1]. This work suggests the need to establish knowledge of fuel properties and thermal decomposition kinetics for energy crop biomass harvested from a phytoremediation project [13,14], which is the primary objective of the study presented in this present paper and can be useful for pyrolysis reactor and process design [15]. Detailed studies on the related phytoremediation-driven energy crop production in the soils contaminated with heavy metals (HMs) and the relationship between the soil chemistry and the bio-productivity has been reported separately [13,14].

2. Materials and methods

2.1. Phytoremediation sites and methods

As presented earlier, the present study focused on the fuel properties and thermal degradation kinetics of the energy crop biomass harvested from a related phytoremediation project [13,14]. Therefore, only a brief of the phytoremediation sites and methods is presented here.

The phytoremediation experiments were conducted outdoors on the heavy metal contaminated (HMC) arable land in Bytom, Poland (Institute for Ecology of Industrial Areas; 50°20′43.0″N 18°57′19.6″E) and a former sewage sludge dewatering site in Leipzig, Germany (Vita34 AG, Business Unit BioPlanta, Deutsche Platz 5, 04103 Leipzig, Germany; 51°25′23.7″N 12°21′56.2″E). The Polish site is an agricultural land contaminated with heavy metals (mainly zinc, cadmium and lead) emitted from a decommissioned smelter plant nearby. The heavy metal contents (Zn, Cd and Pb) of the soil exceed the limits set by the Polish law for arable lands, inducing an exclusion of the soil from food production [14]. The German site is a former sewage sludge dewatering plant that was operational from 1952 to 1990. Following its closure, approximately 650,000 tons of sewage sludge remained in several basins of the area.

Each of the selected sites was divided into three plots of 16 m^2, with a buffer zone of 4 m wide in between to protect the phytoremediation plants against uncontrolled fertilization. To stimulate the uptake of heavy metals by the energy crops and to improve the soil quality, both of the contaminated sites were treated as follows:

- C – Base case as reference, no fertilizer addition.
- NPK- NPK standard fertilization (ammonium sulphate and Polifoska - 4% N, 22% P_2O_5, 32% K_2O), applied directly to the soil before planting, (nitrogen 100 kg ha^{-1}, phosphorus 80 kg ha^{-1} as P_2O_5 and potassium 120 kg ha^{-1} as K_2O).
- INC - Commercial microbial inoculum Emfarma Plus® ProBiotics Poland (Lactic Acid Bacteria $>3.0 \times 10^5$ cfu cm^{-3}, Yeast $< 1.0 \times 10^6$ cfu cm^{-3}, and Purple Non-Sulfur Bacteria $>1.0 \times 10^4$ cfu cm^{-3} in molasses suspension). Eight litres (8 dm^3) of a 10% water solution of Emfarma Plus was used to soak the roots of the seedlings and sprayed on the soil surface. Plant leaves were treated monthly during the growing season with a 10% water solution of Emfarma Plus by aerosol treatment (8 dm^3 per plot).

Miscanthus x *giganteus* and *Sida hermaphrodita* were selected as phytoremediation energy crops planted in both of the contaminated sites. Biomass samples (the whole plant above ground) were collected after the third growing season from three randomly selected plants on each plot which was not exposed to the edge effect.

For site characterization, three composite soil samples per plot (from a depth of 0–20 cm) were collected before starting the experiment and after the third growing season along with plant biomass samples when the bioavailability of heavy metals in the soil was determined. Soil properties including soil texture, pH, electrical conductivity, content of organic matter, total metal concentration (*aqua regia* extraction) and bioavailable fractions of heavy metals ($CaCl_2$ extraction) were determined for the collected soil samples. The pH value was measured in H_2O (1:2.5 m/v) with a glass/calomel electrode (OSH 10-10, METRON, Poland) and a pH-meter (CPC-551, Elmetron, Poland) at 20 °C. The electrical conductivity was determined by an ESP 2 ZM electrode (EUROSENSOR, Poland) according to the Polish standard [16]. The soil texture was evaluated using a hydrometric method, according to the Polish standard [17]. The bioavailability of heavy metals in the soils was studied by means of the extraction method using 3 g of air-dried soil digested in 30 cm^3 of 10 mol m^{-3} $CaCl_2$ solution for 2 h. The concentration of heavy metals in the extracted samples was measured by means of a flame atomic absorption spectrophotometry (Varian Spectra AA300). Results from the soil characterization are presented in Table 1.

2.2. Fuel characterization methods

The moisture content of biomass was determined according to the European Standard EN 15934:2012. The ash content was determined by burning an amount of 1 g sample of all studied solid recovered fuels in a muffle furnace at 250±10 °C for 50 min and then at 550±10 °C for 4 h, according to the EN 15403:2011 European Standard. The volatile matter was determined by maintaining 1 g samples at 900±10 °C for 7 min, according to the EN 15402:2011 method. The ultimate analysis (carbon, hydrogen and nitrogen content) was performed using an Elemental Analyzer from Leco, LECO CHN628. The heavy metal content was measured by means of a Perkin Elmer Elan DRC II inductively coupled plasma mass spectrometer.

The thermal decomposition of the *Miscanthus* x *giganteus* and *Sida hermaphrodita* biomass samples harvested from the phytoremediation project was studied by means of a thermogravimetric (TG) analyser, Netzsch STA 409, operated non-isothermally in N_2/CO_2 (80/20 in volume) atmosphere (80 cm^3 min^{-1}), at a constant heating rate of 10 K min^{-1} up to 850 °C. For each TG analysis run, an amount of approx. 5 mg dry biomass with particle sizes smaller than 500 μm was used. The choice of the atmosphere used for the TG analysis was based on practical considerations relevant to possible flue gas utilizations for a better economy of biomass pyrolysis and torrefaction [18].

Table 1
Chemical and physical properties of the contaminated soils.

Parameter	Polish Site	German Site
pH (1 : 2.5 soil/KCl ratio)	5.94–6.55	6.19–6.50
Electrical conductivity (μS cm^{-1})	77–117	484–1495
Organic matter content[a], % w/w	4.0–7.08	28.3–39.7
Sand fraction[b] (1–0.05 mm), % mass	28	58
Silt fraction[b] (0.05–0.002 mm), % mass	56	19
Clay fraction[b] (<0.002 mm), % mass	16	23
Total heavy metal concentration (extraction with *aqua regia*)		
Pb (mg kg^{-1})	362.3–639.1	474.0–686.0
Cd (mg kg^{-1})	13.69–26.29	25.70–36.39
Zn (mg kg^{-1})	1300–2498	2974–4044
$CaCl_2$ extractable metal fraction[c]		
Pb (mg kg^{-1})	BDL	BDL
Cd (mg kg^{-1})	0.349–1.928	0.220–0.460
Zn (mg kg^{-1})	9.26–112.47	3.45–25.60

[a] Mass fraction of the organic matter in the soil on a dry basis.
[b] Mass fraction of the minerals (Sand, silt, clay) in the soil on a dry and organic matter free basis.
[c] Extraction with 10 mol m^{-3} $CaCl_2$.

2.3. Methods and assumptions for kinetic modelling

A global kinetic model with three parallel reactions adopted from the literature [19–26] was employed for the kinetic modelling. One advantage of this model is that it does not require testing the fuel at different heating rates. Moreover, the model can well describe the separate decompositions of the three main components of lignocellulosic biomass including hemicellulose, cellulose, and lignin [19–26]. The three independent parallel reactions used in this work are:

$$A_v \rightarrow V_1 \quad (1)$$

$$B_v \rightarrow V_2 \quad (2)$$

$$C_v \rightarrow V_3 \quad (3)$$

where A_v, B_v, and C_v are the three pseudo-components; and V_i ($i = 1, 2, 3$) is the total volatiles released from the pyrolysis of the respective pseudo-components. The conversion rates of all reactions follow the Arrhenius expression (Eq. (4)):

$$\frac{d\alpha_i}{dt} = A_i \exp\left(-\frac{E_i}{RT}\right)(1-\alpha_i)^{n_i}, \quad i = 1, 2, 3 \quad (4)$$

where A is the pre-exponential factor, E is the activation energy of the reaction, R is the universal gas constant, T is the absolute temperature, n is the reaction order, and i means the ith pseudo-component. The conversion degree (α) is defined by Eq. (5) as the mass fraction of the decomposed solid or released volatiles:

$$\alpha = \frac{m_0 - m}{m_0 - m_f} = \frac{v}{v_f} \quad (5)$$

where m_0 and m_f are the initial and final masses of the solid, m is the mass of the solid at any time; v_f is the total mass of released volatiles and v is the mass of released volatiles at a given time.

The overall conversion rate is the sum of the partial conversion rates, where c_i indicates the contribution factor or the volatile fraction produced from each component in the following equation:

$$\frac{d\alpha}{dt} = \sum_{i=1}^{3} c_i \frac{d\alpha_i}{dt} \quad (6)$$

The curves fitting operation was based on the non-linear least squares method, in which the objective function to be minimized is:

$$S = \sum_{j=1}^{N} \left[\left(\frac{d\alpha_j}{dt}\right)_{exp} - \left(\frac{d\alpha_j}{dt}\right)_{cal}\right]^2 \quad (7)$$

where $\left(\frac{d\alpha_j}{dt}\right)_{exp}$ and $\left(\frac{d\alpha_j}{dt}\right)_{cal}$ represent the experimental and calculated conversion rates, respectively, and N is the number of experimental points. The fit between measured and simulated values is defined by Eq. (8) as:

$$Fit\ (\%) = \left(1 - \frac{\sqrt{\frac{S}{N}}}{\left[\left(\frac{d\alpha_j}{dt}\right)_{exp}\right]_{max}}\right).100\% \quad (8)$$

The curve fitting process was run until a best fit between the simulated data and the experimental results was obtained. Then, kinetic parameters can be extracted, including: the activation energies (E_1, E_2, E_3), the pre-exponential factors (A_1, A_2, A_3), the contribution factors (c_1, c_3, c_3), and the reaction orders (n_1, n_2, n_3). Conventionally, the names of pseudo-component 1, 2, and 3 are assigned to hemicellulose, cellulose and lignin, respectively.

3. Results and discussion

3.1. Proximate and ultimate analysis

The fuel properties including data from the proximate and ultimate analysis of *Miscanthus* x *giganteus* (MG) and *Sida hermaphrodita* (SH) are summarized in Table 2. The data includes the content of elemental carbon, hydrogen, nitrogen and oxygen as well moisture with ash and volatile matter content, for the Polish and German samples. Some differences between the reference samples of *Miscanthus* x *giganteus* and *Sida hermaphrodita* are observed. For both sites, the ash content of MG_R samples is higher than that of SH_R samples. This suggests that *Miscanthus* x *giganteus* was able to uptake more heavy metals than *Sida hermaphrodita*. This trend is also valid of the cases of NPK or INC addition. It is interesting to see that the ash contents of all samples from German site are higher than the counterparts from Polish site, which is probably due to among others the lower pH value (more acidic, dissolving more metal compounds for plants to uptake) and higher content of heavy metals of the German soil compared to the Polish soil (Table 1), except for the case of SH_{INC}. The reason for the SH_{INC} case is unclear, but it is even more interesting to observe from Table 2 that the sample SH_{INC} from the Polish site is the only case having a positive effect of inoculation on the ash content (4.8% wt.), compared to the reference (2.7% wt.).

3.2. Themogravimetric analysis

The themogravimetric analysis (TGA) was performed for 12 biomass samples of the studied energy crops in identical conditions as described in section 2.2. Fig. 1 represents the TGA data and its derivative form (DTG) for the biomass samples of *Sida hermaphrodita* harvested from the two sites under investigation, Polish and German sites. In general, each of the TGA curves can be divided into three distinguished parts, corresponding to three specific stages of the thermal decomposition process. First, the drying stage was taking place at temperatures up to 200 °C, where the mass loss was caused mainly by the reduced moisture content of the biomass. The second stage was pyrolysis, which started at around 200 °C and ended approximately at 350 °C. In this stage, the mass loss was caused by the release of volatile matters into the gas phase. This is the reason why this stage is also known as "*devolatilisation*" stage. The last stage lasting from 400 °C until the end of the TG analysis was the further thermal decomposition associated with char formation and

Table 2
Proximate and ultimate analysis of collected biomass samples.

% mass	Polish site					
	MG_R	MG_{NPK}	MG_{INC}	SH_R	SH_{NPK}	SH_{INC}
C^{daf}	46.90	45.50	46.50	46.20	46.40	47.00
H^{daf}	7.32	6.88	7.13	6.69	7.22	7.06
N^{daf}	1.38	1.13	1.49	0.43	0.38	0.30
O^{daf}	44.20	46.29	44.68	46.48	45.80	45.44
Moisture content	8.60	8.30	8.20	9.80	9.10	9.40
Volatile matter^{daf}	74.90	76.50	75.30	75.80	76.90	76.60
Ash^{d}	5.50	4.20	4.90	2.70	2.40	4.80
German site						
	MG_R	MG_{NPK}	MG_{INC}	SH_R	SH_{NPK}	SH_{INC}
C^{daf}	45.40	44.60	45.20	44.10	44.90	44.60
H^{daf}	7.28	6.96	6.84	7.22	6.77	6.96
N^{daf}	2.15	2.06	1.47	0.38	0.65	0.66
O^{daf}	45.17	46.18	46.29	45.80	48.45	47.29
Moisture content	8.20	8.00	8.00	8.90	8.50	9.400
Volatile matter^{daf}	74.00	74.40	74.30	74.10	74.30	75.70
Ash^{d}	6.50	6.30	5.80	3.90	2.80	3.30

MG - *Miscanthus x giganteus*; SH - *Sida hermaphrodita*; R – Reference, no treatment.
NPK – standard fertilization; INC - Commercial microbial inoculum.
^{daf}: dry and ash free.
^{d}: dry.

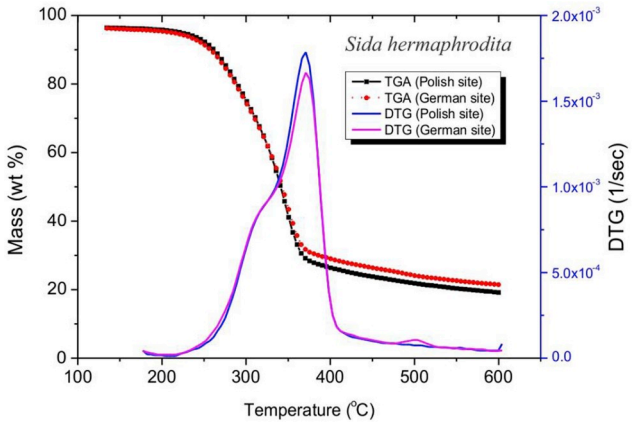

Fig. 1. Site influence on thermal behaviour of the SH reference sample.

synthesis.

From Fig. 1, no significant differences can be observed for the first two stages of the TGA curves. However, the difference is pronounced for the third stage, suggesting a negative effect of the ash content on the biomass reactivity. This difference is in agreement with the data of ash content in Table 2, of which the earlier (ash content) is directly linked to the lower content of heavy metals for the samples from the Polish site (Table 1). In addition, the DTG curve of the sample from the German site has a lower peak than that of the corresponding one from the Polish site. Similar trends are observed for the data collected from the biomass samples (harvested from the two sites under investigation) of *Miscanthus* x *giganteus* and therefore not presented here in this section, which will be included in the kinetic analysis. Instead, Fig. 2 and Fig. 3 represent the effect of fertilization and inoculation on the thermal behaviour of *Miscanthus* x *giganteus* and *Sida hermaphrodita* samples, respectively, harvested from the German site. Similarly, no significant differences among for the TGA curves of R, NPK, and INC samples can be observed from Fig. 2. However, clear differences are observed for the third stage of the TGA curves in Fig. 3. It is interesting to see that the highest reactivity is observed for the SH_{NPK} sample, which follows by that of the SH_R and SH_{INC} samples. On the other hand, while the inoculation resulted in an increase in the ash content of *Sida hermaphrodita* as can be seen in Table 2, a decrease in the ash content is observed for the fertilization.

3.3. Kinetic analysis

The kinetic modelling assuming the three-pseudocomponent model

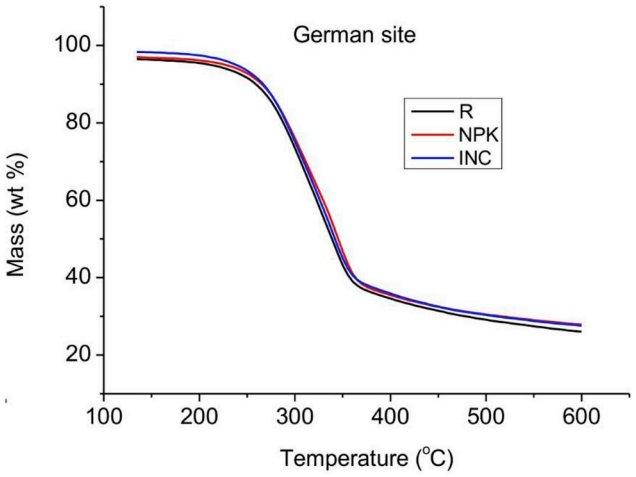

Fig. 2. Influence of fertilization and inoculation on thermal behaviour of *Miscanthus x giganteus* biomass – German site.

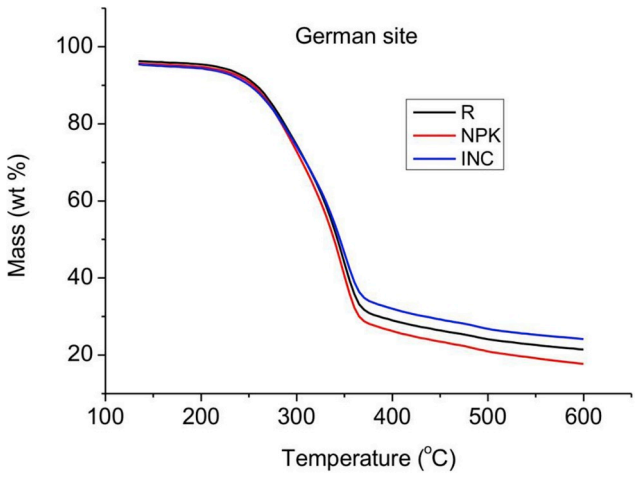

Fig. 3. Influence of fertilization and inoculation on thermal behaviour of *Sida hermaphrodita* biomass – German site.

presented early (Section 2.3) was carried out for the thermal decomposition data collected from the themogravimetric analysis of the biomass samples of the studied energy crops. The kinetic analysis was performed for 12 experimental sets, of which 6 are for the Polish site and 6 for the German site. Results from the kinetic modelling and analysis are presented graphically in Fig. 4 in forms of DTG (Derivative Thermogravimetric) curves, which show good fits between the experimental and calculated results. The kinetic data are numerically extracted and summarized in Table 3.

3.4. Discussion

As presented in Table 3, all the parameters extracted from the kinetic analysis for the studied biomass material are realistic and within reasonable ranges [19–27]. The fit qualities of the curve fittings are within 94.89–99.60%, of which some are relatively low but still reasonable [21,28], co-considering that confidence interval of 95% is widely acceptable in statistics. The reaction order in most of the cases is close to unity, except for lignin (all samples) and hemicellulose of samples 7–9. The activation energies are within 20–103.55 kJ mol^{-1}, which are also relatively low, but within reasonable ranges [19–27]. Among the three pseudo-components, the activation energy of lignin in all cases is within 20–57.11 kJ mol^{-1}, being the smallest, followed by 52.40–100.87 kJ mol^{-1} and 100.21–103.55 kJ mol^{-1} for hemicellulose and cellulose, respectively. This suggests that lignin started decomposing at early stages (relatively low temperatures, around 200 °C). However, the conversion rate of lignin is also low (below $0.2{\cdot}10^{-3}$ s^{-1}), making the lignin curves flat and long. As a result, the lignin curves make the main contributions to the tails of the total curves as shown in Fig. 4. In contrast, the activation energy of cellulose in all cases is the highest. It means that cellulose started decomposing at later stages (relatively high temperatures). However, the conversion rate of cellulose increased and decreased quickly when the increasing temperature programme was proceeding, producing narrow component curves for cellulose with the highest peaks.

For the base cases (1, 4, 7, and 10), the Polish soil seemed producing MG biomass with lower pyrolysis activation energies, whereas an opposite trend is observed for the SH samples. When NPK was added, the activation energies increased, except for cellulose of the SH and Polish MG samples. On the other hand, the effect of inoculation on the activation energy was more complicated.

Overall, Fig. 4 indicates that the energy crops from the Polish site exhibited higher conversion rates than the samples from Germany. This suggests a negative effect of the ash content on the biomass reactivity, co-considering the ash content data in Table 1. The NPK addition

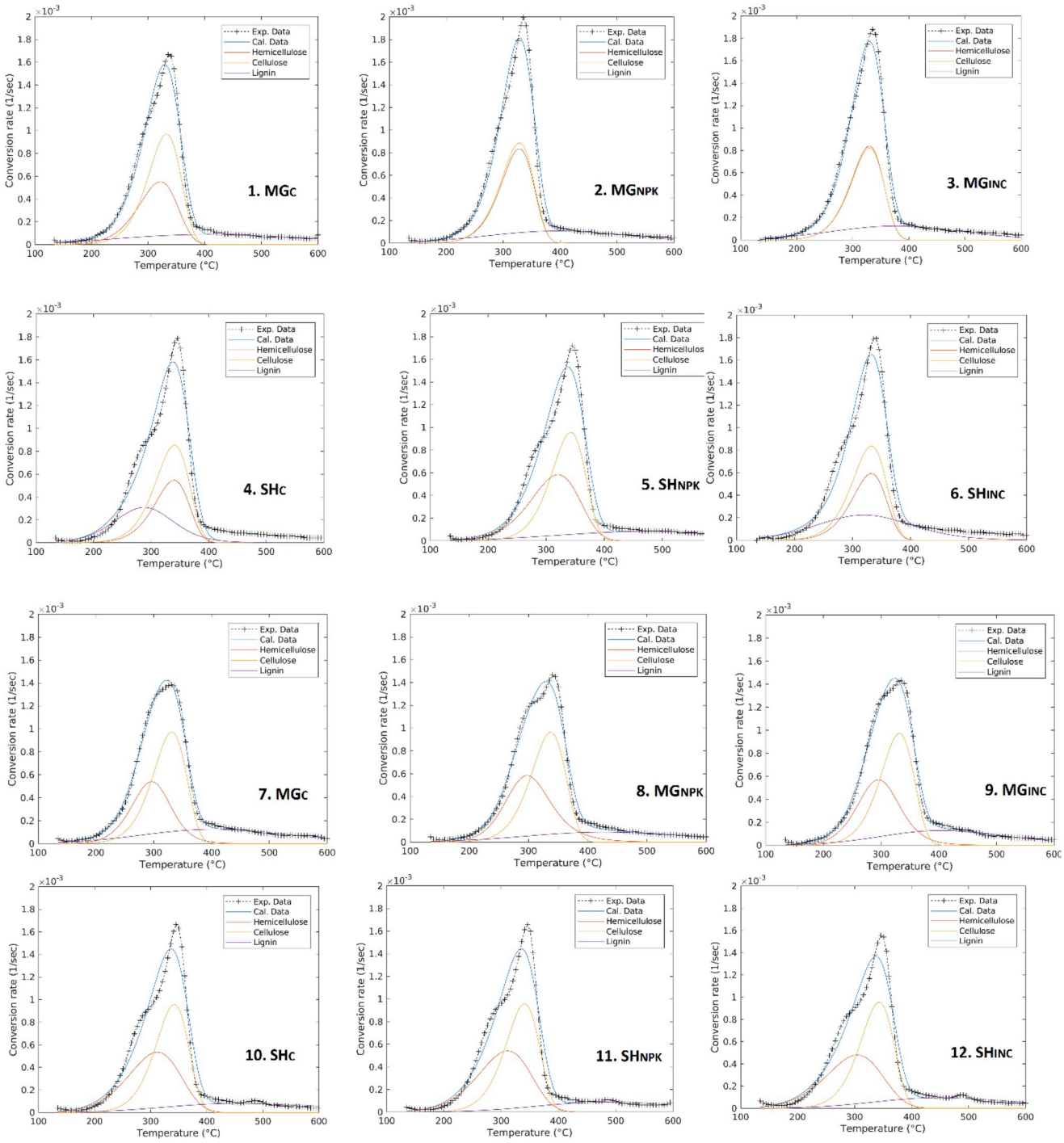

Fig. 4. Optimized DTG curve fitting for 12 data sets (MG - *Miscanthus x giganteus*; SH - *Sida hermaphrodita*; R – Reference, no treatment; NPK – standard fertilization; INC - Commercial microbial inoculum).

increased slightly the overall conversion rate of MG sample (case 2 and 8 compared to case 1 and 7, respectively), and decreased slightly the overall conversion rate of SH samples (case 5 and 11 compared to case 4 and 10, respectively). Opposite trends are observed for the effect of inoculation on the conversion rate.

From the available data and above observations it appears not straightforward to elucidate the correlation between the thermal behaviour of the biomass samples and the soil properties. However, it was possible that the German soil was overall more acidic and thus had a higher organic matter content and electrical conductivity than the Polish one. In addition, this might be related to the differences in the bioavailability of heavy metals, resulting to the higher uptake of heavy metals on the Polish site. In the case of *Miscanthus* x *giganteus* the highest mass drops of the samples during TG analysis were observed for the samples inoculated for both the Polish and German sites. The biomass samples of *Sida hermaphrodita* decomposed the best after fertilization for the German site samples, while the Polish samples achieved the best results after inoculation.

4. Conclusion

From the data presented and analyzed in this work, it is possible at

Table 3
Kinetic data extracted from the kinetic analysis.

Sample ID	c_1	A_1 (s^{-1})	E_1 kJ mol^{-1}	n_1	c_2	A_2 (s^{-1})	E_2 kJ mol^{-1}	n_2	c_3	A_3 (s^{-1})	E_3 kJ mol^{-1}	n_3	Fit quality (%)
Polish site													
1.MG_R	0.2955	66857	81.545	1.01	0.4399	3.27E+06	101.69	1.01	0.24	0.026398	20	1.45	96.80
2.MG_{NPK}	0.3786	2.85E+06	100.33	1.01	0.3997	3.26E+06	100.99	1.01	0.21	0.13756	26.744	1.24	96.62
3. MG_{INC}	0.3814	2.68E+06	100.2	1.01	0.3755	2.66E+06	100.21	1.01	0.22	0.17179	26.828	1.13	97.44
4. SH_R	0.2556	2.11E+06	100.87	1.01	0.3933	3.26E+06	103.12	1.01	0,25	7.11E+02	57.107	1.44	94.92
5. SH_{NPK}	0.3815	1.97E+03	65.092	1.01	0.4406	3.27E+06	103.39	1.01	0.20	5.42E-02	25.772	1.14	95.34
6. SH_{INC}	0.2736	2.13E+06	99.591	1.01	0.3853	2.54E+06	100.47	1.02	0.28	2.91E+00	36.085	1.31	95.71
German site													
7. MG_R	0.2887	3.27E+06	95.539	1.53	0.4406	3.27E+06	101.47	1.01	0.25	0.17655	28.415	1.37	97.99
8. MG_{NPK}	0.3604	3.27E+06	95.908	1.95	0.4406	3.27E+06	102.58	1.01	0.20	0.16109	29.367	1.60	96.71
9. MG_{INC}	0.3314	1.09E+06	90.52	1.64	0.4406	3.27E+06	101.56	1.01	0.23	1.1045	37.41	1.62	97.54
10. SH_R	0.3815	4.21E+02	57.137	1.01	0.4406	3.27E+06	103.37	1.01	0.20	3.29E-01	34.774	1.99	94.97
11. SH_{NPK}	0.3815	4.95E+02	57.769	1.01	0.4406	3.27E+06	103.18	1.01	0.20	9.60E-01	42.068	1.99	94.89
12. SH_{INC}	0.3602	1.71E+02	52.402	1.01	0.44058	3.27E+06	103.55	1.01	0.20	1.17E+00	40.788	1.99	95.11

MG - *Miscanthus x giganteus*; SH - *Sida hermaphrodita*; R – Reference, no treatment.
NPK – standard fertilization; INC - Commercial microbial inoculum; c_i – mass fraction; n_i – reaction order; A_i – pre-exponential factor; E_i activation energy; i = 1, 2, and 3 for hemicellulose, cellulose, and lignin, respectively.

this stage to draw the following conclusions. *Miscanthus* x *giganteus* was able to uptake more heavy metals than *Sida hermaphrodita*. The addition of NPK or INC did not affect this trend. In addition, the ash contents of all samples from the German site were higher than that of the counterparts from the Polish site, except for the case of SH_{INC}. The differences in pH value and heavy metal content of the soils caused differences in the thermal decomposition. The crops from the Polish site exhibited higher conversion rates than the samples from Germany. In addition, the Polish soil produced MG biomass with lower activation energies, whereas an opposite trend was observed for the SH samples. The addition of NPK to the soils led to increases in the activation energies, except for cellulose of the SH and Polish MG samples. The effect of inoculation on the activation energy was more complicated and needs further studies.

The kinetic parameters extracted from the study are realistic and within reasonable ranges. Overall, the activation energies are within 20–103.55 kJ mol^{-1}. The activation energy of lignin is within 20–57.11 kJ mol^{-1}, followed by 52.40–100.87 kJ mol^{-1} and 100.21–103.55 kJ mol^{-1} for hemicellulose and cellulose, respectively. The reaction orders are within 1.01–1.99. The data can be used as input data for modelling of energy systems as well as reactor and process design.

Acknowledgements

This work was financially supported by the Seventh Framework Programme of European Union [grant number 610797] and the Department of Energy and Process Engineering, Norwegian University of Science and Technology, which are gratefully acknowledged.

References

[1] Y. Jiang, M. Lei, L. Duan, P. Longhurst, Integrating phytoremediation with biomass valorisation and critical element recovery: a UK contaminated land perspective, Biomass Bioenergy 83 (2015) 328–339, https://doi.org/10.1016/j.biombioe.2015.10.013.
[2] H.I. Gomes, Phytoremediation for bioenergy: challenges and opportunities, Environ. Technol. Rev. 1 (2012) 59–66, https://doi.org/10.1080/09593330.2012.696715.
[3] D. Desjardins, N.J.B. Brereton, L. Marchand, J. Brisson, F.E. Pitre, M. Labrecque, Complementarity of three distinctive phytoremediation crops for multiple-trace element contaminated soil, Sci. Total Environ. 610–611 (2018) 1428–1438, https://doi.org/10.1016/j.scitotenv.2017.08.196.
[4] Progress in Management of Contaminated Sites, Europe Environmental Agency, 2007. https://www.eea.europa.eu/data-and-maps/indicators/progress-in-management-of-contaminated-sites/progress-in-management-of-contaminated-1. (Accessed 3 January 2020).
[5] V.C. Pandey, O. Bajpai, N. Singh, Energy crops in sustainable phytoremediation, Renew. Sustain. Energy Rev. 54 (2016) 58–73, https://doi.org/10.1016/j.rser.2015.09.078.
[6] X. Liu, Q. Song, Y. Tang, W. Li, J. Xu, J. Wu, et al., Human health risk assessment of heavy metals in soil–vegetable system: a multi-medium analysis, Sci. Total Environ. 463–464 (2013) 530–540, https://doi.org/10.1016/j.scitotenv.2013.06.064.
[7] M. Summersgill, Remediation Technology Costs in the UK & Europe; Drivers and Changes from 2001 to 2005, Technology VHE, 2005 [1][1].pdf (Assessed 03 January 2020), http://www.eugris.info/newsdownloads/cardiff_paper_190_jan06_edit.
[8] D.J. Glass, Economic potential of phytoremediation, in: I. Raskin, B. Ensley (Eds.), Phytoremediation of Toxic Metals, John Wiley & Sons, New York, 2000, pp. 15–31.
[9] A. Mojiri, L. Ziyang, R.M. Tajuddin, H. Farraji, N. Alifar, Co-treatment of landfill leachate and municipal wastewater using the ZELIAC/zeolite constructed wetland system, J. Environ. Manag. 166 (2016) 124–130, https://doi.org/10.1016/j.jenvman.2015.10.020.
[10] B. Dhir, S. Srivastava, Disposal of metal treated salvinia biomass in soil and its effect on growth and photosynthetic efficiency of wheat, Int. J. Phytoremediation 14 (2012) 24–34, https://doi.org/10.1080/15226514.2010.532180.
[11] A. Sas-Nowosielska, R. Kucharski, E. Małkowski, M. Pogrzeba, J.M. Kuperberg, K. Kryński, Phytoextraction crop disposal - an unsolved problem, Environ. Pollut. 128 (2004) 373–379, https://doi.org/10.1016/j.envpol.2003.09.012.
[12] M. Ghosh, S.P. Singh, A review on phytoremediation of heavy metals and utilization of its byproducts, Appl. Ecol. Environ. Res. 3 (2005) 1–18, https://doi.org/10.15666/aeer/0301_001018.
[13] M. Pogrzeba, J. Krzyżak, S. Rusinowski, S. Werle, A. Hebner, A. Milandru, Case study on phytoremediation driven energy crop production using Sida hermaphrodita, Int. J. Phytoremediation 20 (2018) 1194–1204, https://doi.org/10.1080/15226514.2017.1375897.
[14] M. Pogrzeba, S. Rusinowski, J. Krzyżak, Macroelements and heavy metals content in energy crops cultivated on contaminated soil under different fertilization—case studies on autumn harvest, Environ. Sci. Pollut. Control Ser. 25 (2018) 12096–12106, https://doi.org/10.1007/s11356-018-1490-8.
[15] R.S. Kempegowda, P.V. Selvam Pannir, Ø. Skreiberg, K.Q. Tran, Process synthesis and economics of combined biomethanol and CHP energy production derived from biomass wastes, J. Chem. Technol. Biotechnol. 87 (2012) 897–902, https://doi.org/10.1002/jctb.3696.
[16] PN-ISO 11265, 1997 Soil Quality—Determination of Electrical Conductivity, 1997 (In Polish).
[17] PN-R-04032, 1998—Soil and Mineral Pieces—Soil Sampling and Texture Assessment, 1998 (In Polish).
[18] K.Q. Tran, T.N. Trinh, Q.V. Bach, Development of a biomass torrefaction process integrated with oxy-fuel combustion, Bioresour. Technol. 199 (2016) 408–413, https://doi.org/10.1016/j.biortech.2015.08.106.
[19] Q.V. Bach, K.Q. Tran, Ø. Skreiberg, T.T. Trinh, Effects of wet torrefaction on pyrolysis of woody biomass fuels, Energy 88 (2015) 443–456, https://doi.org/10.1016/j.energy.2015.05.062.
[20] Q.V. Bach, T.N. Trinh, K.Q. Tran, N.B.D. Thi, Pyrolysis characteristics and kinetics of biomass torrefied in various atmospheres, Energy Convers. Manag. 141 (2017) 72–78, https://doi.org/10.1016/j.enconman.2016.04.097.
[21] C. Branca, A. Albano, C. Di Blasi, Critical evaluation of global mechanisms of wood devolatilization, Thermochim. Acta 429 (2005) 133–141, https://doi.org/10.1016/j.tca.2005.02.030.
[22] C. Branca, C. Di Blasi, Global kinetics of wood char devolatilization and combustion, Energy Fuels 17 (2003) 1609–1615, https://doi.org/10.1021/ef030033a.
[23] M. Broström, A. Nordin, L. Pommer, C. Branca, C. Di Blasi, Influence of torrefaction on the devolatilization and oxidation kinetics of wood, J. Anal. Appl. Pyrolysis 96 (2012) 100–109, https://doi.org/10.1016/j.jaap.2012.03.011.
[24] J.A. Conesa, A. Domene, Biomasses pyrolysis and combustion kinetics through n-th order parallel reactions, Thermochim. Acta 523 (2011) 176–181, https://doi.org/10.1016/j.tca.2011.05.021.
[25] J.J. Manyà, E. Velo, L. Puigjaner, Kinetics of biomass pyrolysis: a reformulated three-parallel-reactions model, Ind. Eng. Chem. Res. 42 (2003) 434–441, https://doi.org/10.1021/ie020218p.

[26] J.J.M. Orfão, F.J.A. Antunes, J.L. Figueiredo, Pyrolysis kinetics of lignocellulosic materials - three independent reactions model, Fuel 78 (1999) 349–358, https://doi.org/10.1016/S0016-2361(98)00156-2.
[27] E. Avni, R.W. Coughlin, Kinetic analysis of lignin pyrolysis using non-isothermal TGA data, Thermochim. Acta 90 (1985) 157–167, https://doi.org/10.1016/0040-6031(85)87093-3.
[28] W.-H. Chen, Y.-S. Chu, J.-L. Liu, J.-S. Chang, Thermal degradation of carbohydrates, proteins and lipids in microalgae analyzed by evolutionary computation, Energy Convers. Manag. 160 (2018) 209–219, https://doi.org/10.1016/j.enconman.2018.01.036.